Properties of the Solar Corona above a Polar Coronal Hole during the Solar Minimum in 2007

1. Michael Hahn and Daniel Wolf Savin
2. Enrico Landi and Paul Bryans
3. Mari Paz Miralles

1: Columbia Astrophysics Laboratory
2: US Naval Research Laboratory
3: Harvard-Smithsonian Center for Astrophysics

Abstract

Observations have shown that the latest solar minimum differs from the previous one in 1996-1997 (McComas et al. 2008; Wang et al. 2009). Here we present the analysis of EUV spectra of a north polar coronal hole observed during the recent minimum on 16 November 2007. The data were taken using the Extreme ultraviolet Imaging Spectrometer (EIS) on *Hinode*. Five observations span the coronal hole in the longitudinal direction from the center to the boundary with the quiet Sun corona and extend radially from the solar disk to about 1.2 $R_\odot$. We use the Geometric mean Emission Measure (GEM) approach to determine the plasma emission measure EM and electron temperature T_e. The GEM analysis shows that the observations are nearly isothermal, but there are indications of a small contribution from higher T_e plasma along the line of sight. To investigate the temperature structure in more detail we performed a differential emission measure (DEM) analysis. We also determine upper and lower bounds on the ion temperature T_i using measured line widths. Finally, we compare our results to spectroscopic measurements of polar coronal holes obtained from observations carried out during the previous solar minimum in 1996-1997.

Observations

Observations were carried out with the EIS instrument on *Hinode* (Korendyke et al. 2006; Culhane et al. 2007) shown below (Figs. 1 and 2).

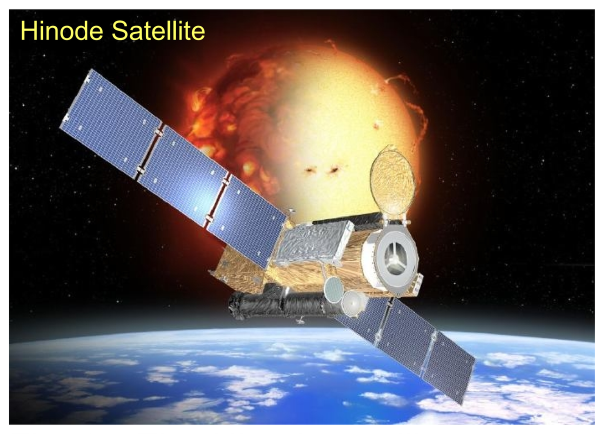

Fig. 1 – The *Hinode* satellite

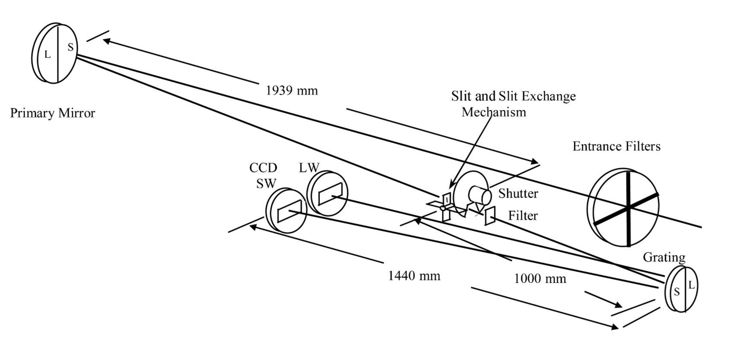

Fig. 2 – EIS (Korendyke et al. 2006)

EIS covers the wavelength ranges 171-211 Å and 245-291 Å with a spectral resolution of 0.022 Å per pixel and instrumental FWHM 0.062 Å for the 2" slit used here (Brown et al. 2008). We analyzed five observations from 2007 November 16. The pointings spanned the polar coronal hole from the center to the edge of the coronal hole. The center of each pointing was at Solar-X = -7", 108", 223", 324", and 423" as shown below (Fig. 3).

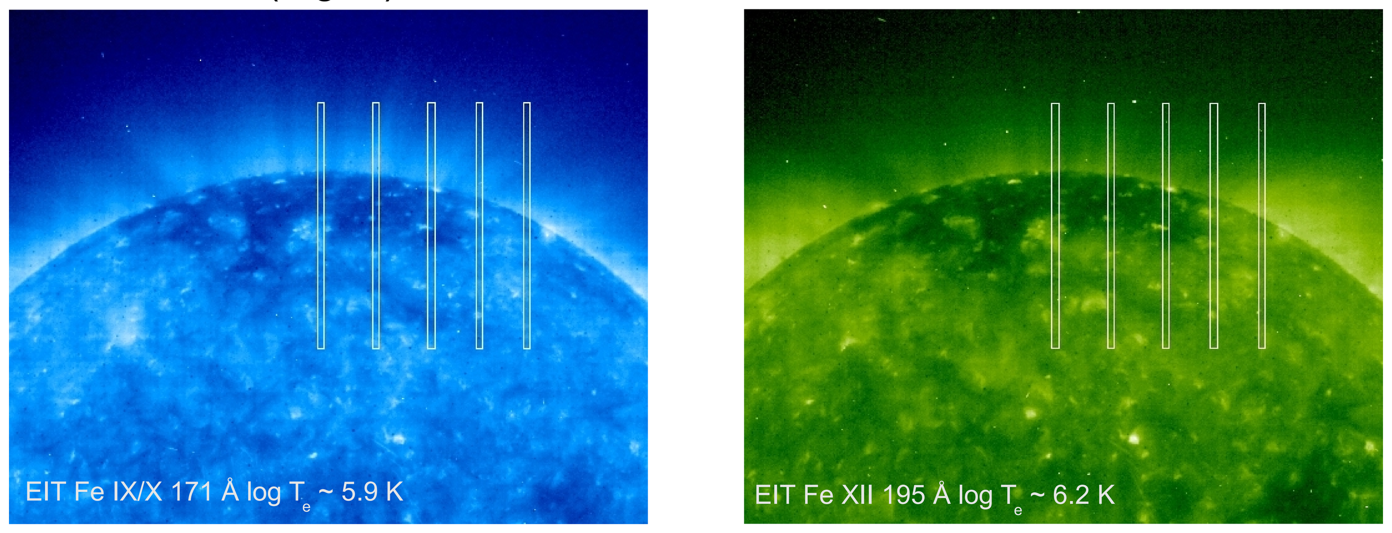

Fig. 3 – EIS slit positions overlayed on *SOHO* Extreme ultraviolet Imaging Telescope images of the polar coronal hole on 2007 November 16.

Each observation covers a 14" x 512" field of view. To improve statistics the pixels were summed into 14" x 10" bins. Only pixels above the solar limb were used in the analysis. Our data set consisted of lines from Fe VIII-XIV; Si VII, IX, and X; S VIII and X; Al VIII and IX; and Mg VII (Fig. 4).

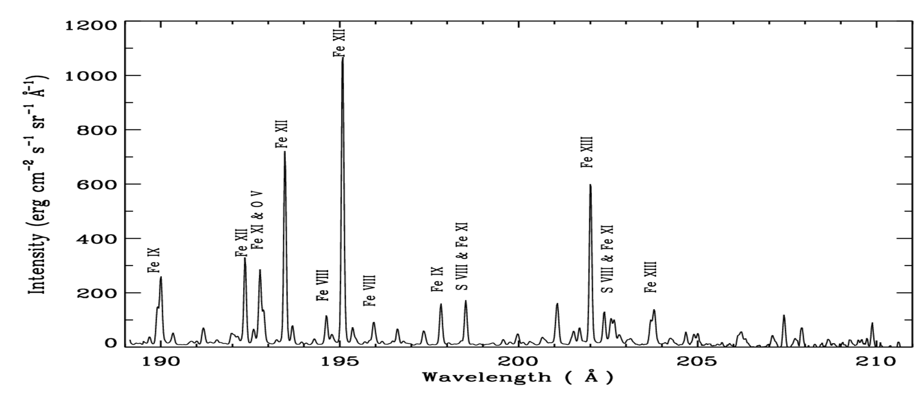

Fig. 4 – Part of the EIS spectrum used in these observations.

Emission line intensities and widths were extracted by fitting Gaussian profiles to the measured spectra (Fig. 5). We used unblended lines, lines where the blended components were separable, and self-blended lines in the analysis. The instrumental scattered light intensity was estimated as 2% of the average intensity on the disk and subtracted (Ugarte-Urra 2010).

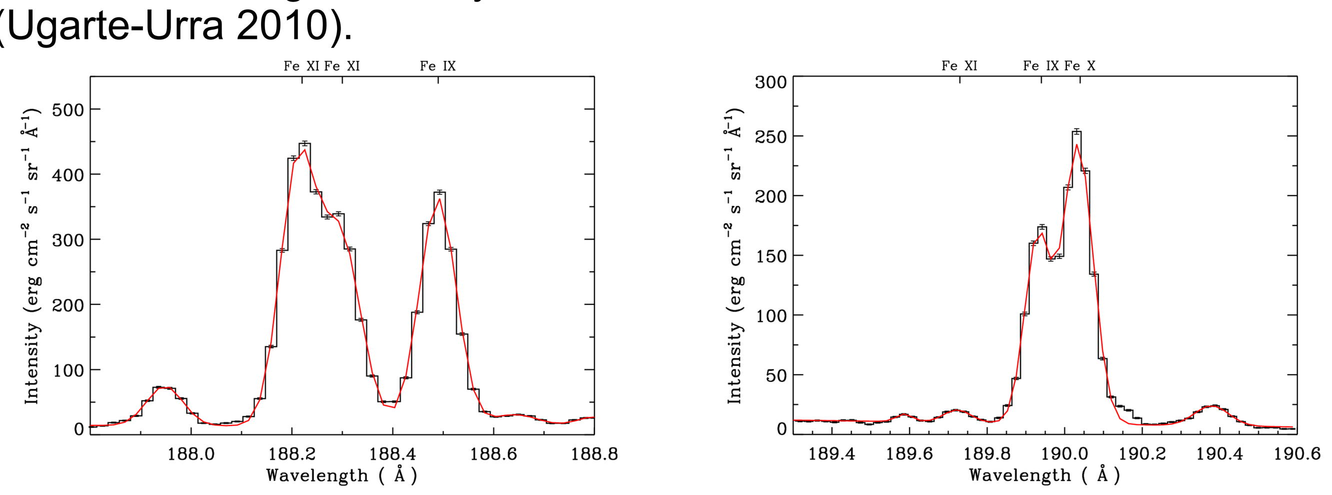

Fig. 5 – Example of a fit to part of the EIS spectrum using a sum of Gaussians. These Fe lines were used in the analysis. Most fits were less complex than these.

Emission Measure Analysis

The GEM method was used to determine T_e, EM, and relative elemental abundances based on measured line intensities (Bryans et al. 2009). The intensity I_{ji} of a radiative transition from level j to i can be described by an integral depending on the density n_e and the contribution function $G(T_e,n_e)$, which contains information about the level populations, ionization equilibrium, elemental abundances, and transition rates.

$$I_{ji}=\frac{1}{4\pi d^2}\int G(T_e,n_e)n_e^2dV \qquad G(T_e,n_e)\equiv\frac{n_j(X^{+q})}{n(X^{+q})}\frac{n(X^{+q})}{n(X)}\frac{n(X)}{n(H)}\frac{n(H)}{n_e}\frac{A_{ji}}{n_e}$$

When the emitting plasma is isothermal and of uniform density, $G(T_e,n_e)$ can be taken out of the integral and the EM

$$\mathrm{EM}\equiv\int n_e^2dV$$

can be found from the measured intensities

$$\mathrm{EM}=4\pi d^2\frac{I_{ji}}{G(T_e,n_e)}\,.$$

Most emission lines are not density sensitive, so that $G(T_e,n_e)$ depends most strongly on T_e and n_e can be fixed in the analysis. Since the EM should be the same for each emission line emitting in the same isothermal volume, T_e and EM are measured by finding the point where all EM(T_e) curves intersect as shown in Fig. 6 below.

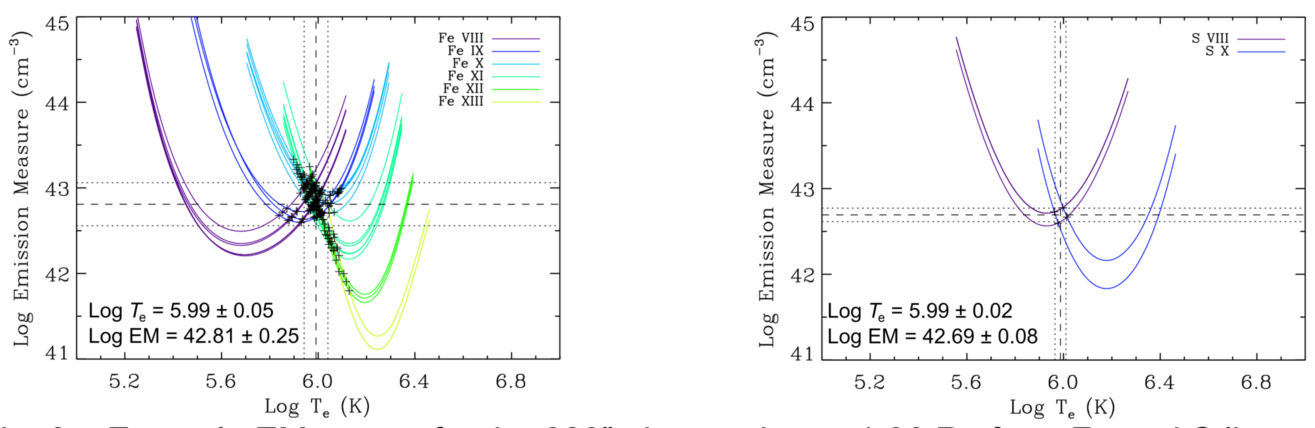

Fig. 6 – Example EM curves for the 223" observation at 1.06 $R_\odot$ from Fe and S lines.

Density

The density was measured using the intensity ratio of density sensitive lines (Fig. 7). Density ratios derived from Fe VIII and IX lines showed that n_e decreases from 8 x 10^7 cm^{-3} to 1 x 10^7 cm^{-3} between 1.05 and 1.15 $R_\odot$. This is about the same as in polar coronal holes during the 1996-1997 solar minimum (Banerjee et al. 1998; Wilhelm et al. 1998; Landi 2008).

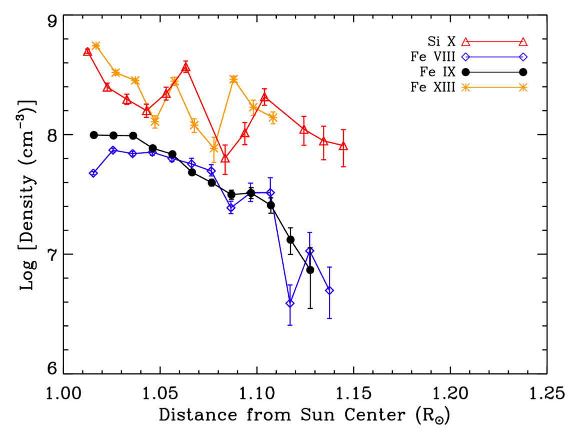

Fig. 7 – Inferred density using different intensity ratios for the 223" observation. The error bars represent statistical errors in the fitting. The fitting errors are underestimated, likely due to fitting the background level for weak lines combined with the sensitivity of the density ratio method to small errors in the intensity. However, the overall uncertainty can be inferred from the scatter in the density profiles.

Si X and Fe XIII lines give a density that is larger than Fe VIII and IX, with a different height dependence. This could be caused by a small amount of quiet Sun corona along the line of sight. Si X and Fe XIII are more abundant at typical quiet Sun temperatures than at coronal hole temperatures. Thus, their line ratios reflect the density of this higher temperature plasma, whereas Fe VIII and IX are insensitive to the higher temperature component. We estimate that the quiet Sun emission measure needs to be only a few percent of the coronal hole emission measure to produce the inferred densities from the Si X and Fe XIII lines.

Electron Temperature

The GEM analysis shows that Log [T_e (K)] increases in the coronal hole from ~5.95 to 6.05 over the height range of these observations (Fig. 8). This agrees with measurements from the 1996 solar minimum (Doschek et al. 1998; Feldman et al. 1998; Doschek et al. 2001; Landi 2008). The 423" observation appears to show a transition from hotter plasma at a temperature typical of the quiet sun corona to cooler coronal hole plasma near 1.15 $R_\odot$.

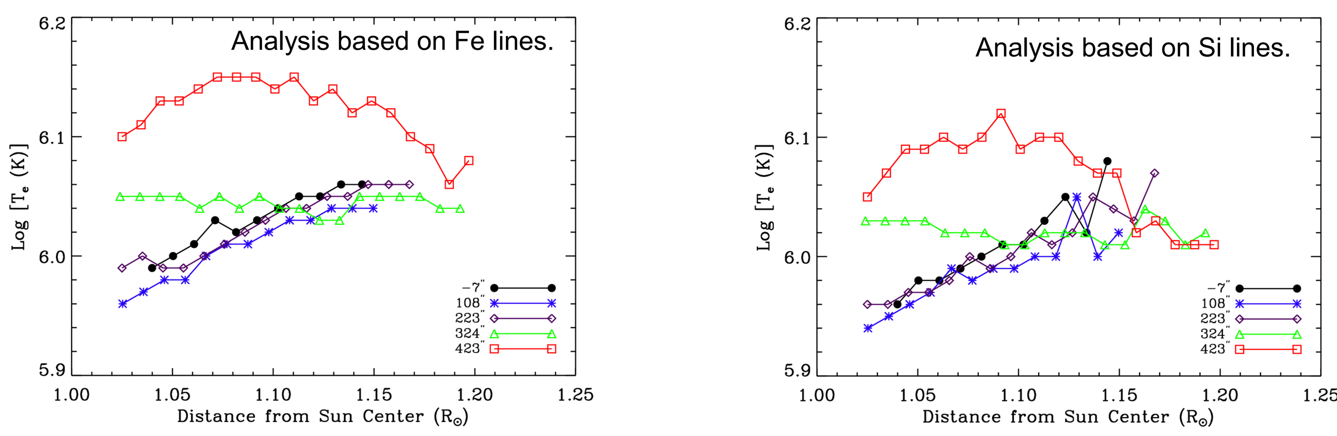

Fig. 8 – Temperature measurements from the GEM analysis of Fe and Si lines. The systematic difference between Fe and Si is caused by the presence in the spectrum of higher charge states of Fe, which form at higher temperatures and tend to raise the average crossing point.

Differential Emission Measure (DEM)

The T_e profiles and n_e measurements could be affected if the observations are not exactly isothermal along the line of sight. We used the iterative method of Landi and Landini (1997) to derive the DEM, $\varphi(T_e)$, defined by:

$$I_{ji}=\frac{1}{4\pi d^2}\int G(T_e,n_e)\phi(T_e)dT_e \qquad \phi(T_e)dT_e=n_e^2dV\,.$$

To find $\varphi(T_e)$ an initial $\varphi_o(T_e)$ is assumed and the predicted intensity is calculated and compared to the measured intensity. $\varphi_o(T_e)$ is then corrected to produce $\varphi_1(T_e)$. Iterations continue until $\varphi(T_e)$ converges.

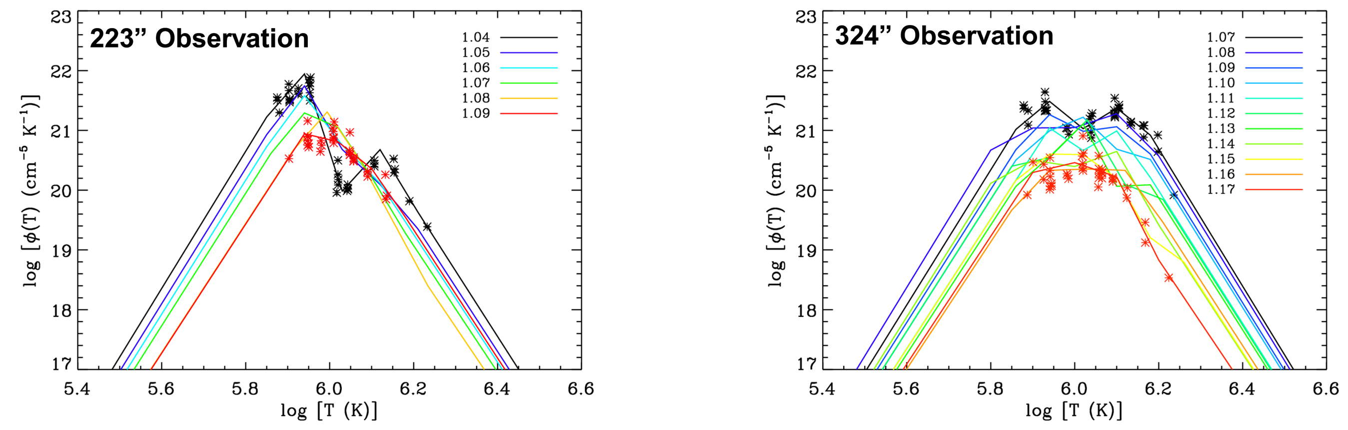

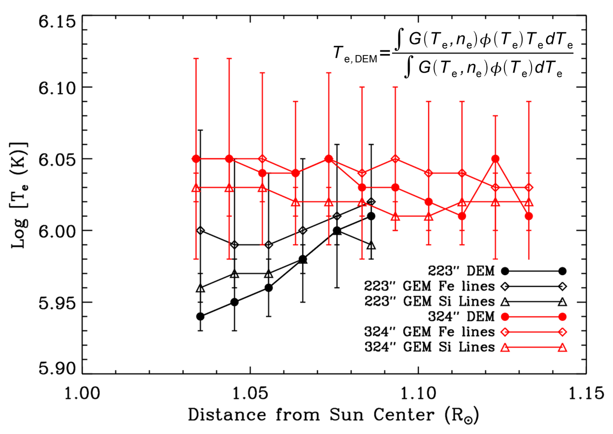

Fig. 9 – DEMs for different heights. Asterisks show the data points derived from analysis of each line for selected heights. The 223" observation (upper left) is nearly isothermal with a small amount of emission coming from higher T_e. At T_e = 5.9 the DEM decreases with height, but is roughly constant near T_e = 6.1. In the 324" observation (upper right) φ has two peaks or one very broad peak and decreases uniformly with height. We calculated a mean temperature from the DEM (lower right) and found that these deviations from isothermality can explain the T_e profiles from the isothermal GEM analysis.

Ion Temperature

Line widths are related to T_i, nonthermal velocities v_{nt}, and the instrumental width

$$\Delta\lambda_{\mathrm{FWHM}}=\left[\Delta\lambda_{\mathrm{inst}}^2+4\ln(2)\left(\frac{\lambda}{c}\right)^2\left(\frac{2k_BT_i}{M}+v_{\mathrm{nt}}^2\right)\right]^{1/2}\,.$$

From the line widths we found the upper bound on T_i by assuming v_{nt} = 0. For the lower bound we initially assumed that T_i=0 for the narrowest line in the dataset and derived an upper bound on v_{nt}. The results were consistent with T_i > T_e. Thus, we adopt the more restrictive assumption T_i = T_e to produce a tighter bound on T_i.

Figure 10 shows the dependence of T_i on the charge-to-mass ratio q/M of the ion. Figure 10 shows how the line widths increase with height. This could be due to more heating, less cooling, or increasing v_{nt}. If v_{nt} is produced by waves then v_{nt}^2 = <δv^2> and v_{nt} could increase with height due to conservation of wave energy F as n_e and B decrease

$$F\approx\sqrt{\frac{n_em_p}{4\pi}}\langle\delta v^2\rangle B\,.$$

The behavior of T_i and v_{nt} is similar to what was found in polar coronal holes for the 1996-1997 solar minimum (Banerjee et al. 1998; Doschek et al. 2001; Landi & Cranmer 2009).

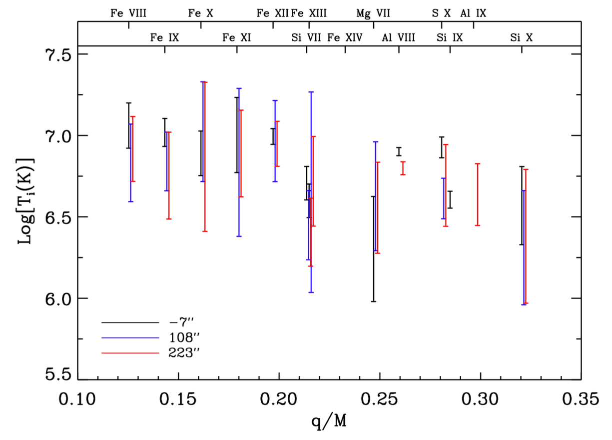

Fig. 10 – T_i bounds for the -7", 108", and 223" observations at 1.05 $R_\odot$. The x-axes of the plots have been shifted slightly for clarity.

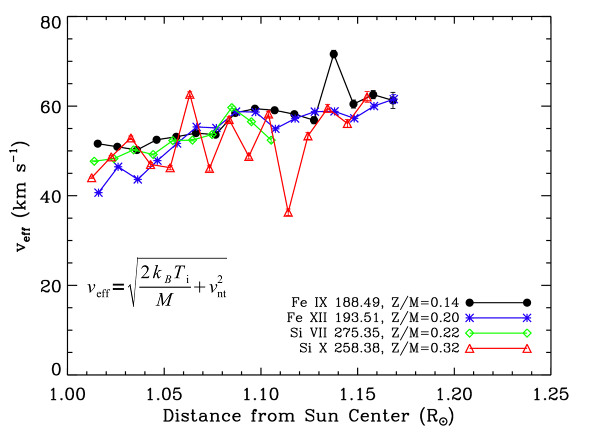

Fig. 11 – Line width expressed as the effective (thermal plus non-thermal) velocity versus height in the 223" observation.

Summary

We found broad similarities between the properties of this polar coronal hole at low altitudes during the recent solar minimum and similar measurements of polar coronal holes for the 1996-1997 minimum. The electron temperature T_e, the gradient of T_e, T_i, the T_i dependence on q/M, and increasing line widths with height were all similar to during the previous minimum. A DEM was performed, which showed that although the observation is approximately isothermal, some emission comes from a higher T_e component. This influences our T_e and n_e results.

References

Banerjee D., et al., 1998, A&A, 339, 208.
Bryans P., et al., 2009, ApJ, 691, 1540.
Culhane, J. L., 2007, Sol. Phys. 243, 19.
Doschek, G. A., et al., 1998, ApJ, 504, 573.
Doschek, G. A., et al., 2001, ApJ, 546, 559.
Landi, E., 2008, ApJ, 685, 1270.
Landi, E. and Landini, M., A&A, 327, 1230, 1997
Landi, E., and Cranmer, S.R., 2009, ApJ, 691, 794.
McComas, D. J., et al., 2008, Geophys. Res. Lett., 35, L18103.
Ugarte-Urra, 2010, Private Communication
Wang, Y.-M., et al., 2009, ApJ, 707, 1372.
Wilhelm, K., et al., 1998, ApJ, 500, 1023.